Current Science
CS 5 (4), 3420-3431 (2025)
Received 16 April 2025 | **Revised 06 May** 2025 | **Accepted 10 June**. 2025 | **Online Available 02 July** 2025
https://doi.org/ 10.52845/CS/2025-5-4-8

Current Science

Current Science

OPEN ACCESS

ISSN(O)2795-8639

Original Article

Sculptouch: A Study on Distributed Flexible Capacitive Haptic Sensing with Neural-Enhanced Gesture Recognition for High-Fidelity Virtual Reality Interaction

Jian Teng[1,2] ; Sukyoung Cho[2],* Shaw-mung Lee[3]

[1]School of Mechanical and Electrical Engineering, Lingnan Normal University, Zhanjiang, China

[2]College of Education, Sehan University, Yeongam, Jeollanam-do, Republic of Korea

[3]Technology Research Institute, Arrow Technology Company, ZhuHai, China

[*]Corresponding Author: Sukyoung Cho

Abstract:
Virtual reality sculpting tools currently lack the tactile feedback essential for teaching material manipulation skills in sculptural education, limiting their pedagogical effectiveness compared to traditional hands-on training. This study presents SculpTouch, a haptic interface system that addresses this gap through distributed force sensing using finger-mounted capacitive sensor arrays (4×4 electrodes) sampling at 40 kHz. The system implements a three-phase modeling workflow mimicking traditional clay sculpting: form stroking through palm pressure, material carving with precise finger movements, and detail pinching using thumb-index coordination. Neural network processing combining convolutional layers and bidirectional LSTMs enables real-time gesture recognition. SculpTouch achieved 0.38 mm spatial accuracy, sub-4 ms latency, 0.01 N force resolution, and 94.8% gesture classification accuracy across 25 participants. The system successfully distinguishes compression and tension zones during forming operations and maintains consistent parting lines during detail work, enabling authentic sculptural skill development in virtual environments previously impossible with existing VR tools.

Keywords: Flexible sensing; Virtual reality; Haptic interface; Neural networks; Gesture recognition; Sculptural education

1. Introduction

Virtual reality revolutionizes 3D modeling education, yet current tools fail to replicate the tactile learning essential for sculptural skill development. Tilt Brush, Google's pioneering VR painting application launched in 2016, transforms rooms (Blazheva, 2021)into canvases where users paint with light, fire, and stars in three-dimensional space. While visually spectacular, its stroke-based approach lacks the force feedback crucial for teaching material manipulation. Educational comparisons reveal Tilt Brush functions more as 3D installation art than traditional sculpting, missing fundamental features like pressure-sensitive material deformation (Myoo, 2022).

Professional alternatives emerged addressing specific limitations. Gravity Sketch differentiates itself through precision tools for professional 3D modeling, moving beyond artistic expression togenuine design workflows (Lin et al., 2025). However, even Gravity Sketch's advanced surface controls and export capabilities cannot convey the resistance students must learn when shaping physical materials (Jaafar et al., 2024). Oculus Medium offers voxel-based sculpting that approximates clay manipulation, allowing users to "spray" geometry and carve volumes, yet provides only binary collision feedback through controller vibration (Myoo, 2022).

The pedagogical gap becomes evident in

classroom deployment. Ho et al. (2019) found that while VR painting tools increased student motivation for 3D animation learning, the absence of haptic feedback limited skill transfer to physical media (Serna-Mendiburu & Guerra-Tamez, 2024). Students struggle translating vibration patterns into meaningful force application—a critical component of sculptural technique. Current creative VR tools span painting, modeling, and animation, yet none adequately address the force-based learning requirements of sculpture education (Ho et al., 2019).

This limitation constrains VR's educational potential. Architecture and medical training successfully adopted VR because visual and procedural learning suffice. Sculpture demands proprioceptive education—understanding material resistance, developing muscle memory for appropriate force application, and learning through physical failure. Without authentic haptic feedback, VR sculpting remains an abstraction unsuitable for foundational skill development.

Research demonstrates that kinesthetic force feedback significantly enhances learning outcomes compared to vibrotactile alternatives, particularly for motor skill acquisition (Li et al., 2024). This paper presents SculpTouch, addressing this critical gap through distributed force sensing that captures the complete hand-material interaction, enabling authentic sculptural education in virtual environments.

2. Related Works

2.1 Haptic Sensing Technologies for VR Applications

Recent advances in haptic interfaces for VR have explored diverse sensing mechanisms. Shi and Shen (2024) categorized haptic sensing approaches into piezoresistive, capacitive, piezoelectric, and triboelectric mechanisms, identifying capacitive sensing as optimal for spatial resolution despite force range limitations(Shi & Shen, 2024). Wang et al. (2022) developed augmented tactile rings with triboelectric sensors for metaverse applications, though limited to gesture recognition rather than continuous force measurement (Sun et al., 2022). Lu et al. (2023) demonstrated that optimizing electrode arrangement and surface microstructure density significantly enhanced signal quality for dynamic touch decoding using machine learning (Lu et al., 2023).

2.2 Neural Network Architectures for Tactile Processing

Deep learning has transformed tactile data processing. Tsuji and Kohama (2019) applied CNNs to roughness recognition, achieving 85% accuracy but requiring fixed scanning speeds(Tsuji & Kohama, 2019b). Zapata-Impata et al. (2019) advanced this through 3D CNNs processing pressure image sequences as tensors, achieving 92% classification accuracy for robotic palpation (Pastor et al., 2019). Suresh et al. (2023) combined visual and tactile perception through neural fields for in-hand manipulation, demonstrating robust object tracking (Suresh et al., 2024). Recent hybrid triboelectric- capacitive sensors with deep learning achieved 98.46% object recognition accuracy through multimodal signal fusion (Xie et al., 2024).

2.3 Virtual Sculpting and Creative Applications

Virtual sculpting demands exceptional haptic fidelity. Blanch et al. (2004) pioneered non-realistic haptic feedback for virtual sculpture using implicit surface scalar fields. Commercial systems like Geomagic Sculpt employ single-point haptic styluses for organic modeling, though lacking full- hand interaction capabilities . Li et al. (2024) showed kinesthetic gloves significantly enhanced body ownership and agency in VR compared to vibrotactile feedback alone (Li et al., 2024).

2.4 Force Sensing and Multimodal Integration

Wang et al. (2023) identified capacitive sensing as optimal for static force measurements while emphasizing hybrid approaches for dynamic scenarios (Jin et al., 2023). Singh et al. (2024) demonstrated distributed finger sensing could compensate for mechanical constraints in under-actuated hands through intelligent processing (Singh et al., 2024). Recent perspectives emphasize haptic interfaces must provide fast response, light weight, and both tactile and kinesthetic feedback for immersive metaverse experiences (Tang et al., 2024).

Pezent et al. (2023) showed multisensory pseudo-haptics combining visual cues with wrist-based feedback could enhance illusions with simplified hardware (Pezent et al., 2023). Venkatesan et al.

(2023) found that compared to pure tactile conditions, force feedback significantly enhances emotional responses in virtual environments(Venkatesan et al., 2023). Jung and their team (2024) proposed an action-tactile framework for improving VR performance, which has inspired our research approach to extracting gesture features(Jung et al., 2024).

These advancements together highlight a key set of insights: effective haptic interaction interfaces demand multimodal perception, refined signal processing, and careful attention to perceptual elements that extend beyond mere force measurement. However, our research has uncovered critical shortcomings—foremost among them the absence of distributed finger-level force sensing capability, and the lack of customized integrated solutions tailored to creative applications requiring fine manual control. By integrating high-resolution capacitive sensor arrays with bio- inspired neural processing techniques, we present a viable path to preserving the richness of physical interaction in virtual environments.

3. Methods and Materials

3.1 System Architecture and Hardware Design

3.1.1 Wearable Multi-modal Sensing Platform

The SculpTouch system employs flexible sensors mounted on the fingers to capture force and spatial interaction data from individual digits during virtual sculpting. Each of the five finger-mounted sensors consists of a 4×4 capacitive electrode array, fabricated on a flexible polyimide substrate dimensioned to conform to finger anatomy (15×20 mm).The capacitive sensing is managed by a Cypress CY8CMBR3116 controller, which provides the necessary sensitivity for detecting subtle pressure variations during sculpting gestures.

The system achieves force resolution of 0.01 N per finger through Texas Instruments FDC2214 capacitance-to-digital converters sampling at 40 kHz. This high sampling rate ensures capture of rapid sculpting movements without loss of detail. Power consumption was optimized for extended use, with the complete system drawing 180 mW during active operation from an 800 mAh battery, enabling approximately 4 hours of continuous sculpting sessions.

3.1.2 Virtual Reality Integration

Integration with commercial VR headsets (Meta Quest 2, HTC Vive Pro 2) was accomplished through OpenXR SDK to ensure broad compatibility. The system combines optical tracking from the VR headset with supplementary IMU data (MPU-9250) to enhance hand position accuracy, particularly important during fine detail work. This multi-sensor fusion approach reduces tracking errors that typically occur when hands occlude the headset's optical sensors.

The virtual sculpting environment runs at 90 Hz to match the VR display refresh rate, preventing motion sickness and ensuring responsive haptic feedback. Mesh deformation calculations are executed on the GPU, ensuring real-time performance even when processing complex models.

3.1.3 Three-Phase Modeling Workflow

The system is designed around three distinct interaction stages, strictly following the intuitive workflow of traditional clay sculpting:

Phase 1 : Initial shapes are created through broad sweeping motions of the palm, utilizing pressure-driven deformation to establish basic forms.

Phase 2: Precise material removal is achieved via fine finger movements combined with Boolean operations, enabling detailed cutting and shaping.

Phase 3 : Fine details and surface textures are sculpted through coordinated movements of the thumb and index finger, enhancing the model's intricacy.

The force-contact relationship follows(Arshad et al., 2024).

$$= = \quad 0 \; - \; 0 \; \frac{+ F + F^{1.5}}{_0 - F}$$

Where:

- *C = capacitance (pF)*

- *ε0= permittivity of free space (8.854 × 10⁻¹² F/m)*
- *εr = relative permittivity*
- *A= contact area (mm²)*
- *F= applied force (N)*
- *d= electrode gap (mm)*
- *α=12.5, β=0.45, γ=0.0009 (experimentally calibrated coefficients)*

Each Phase employs distinct signal processing strategies tailored to its specific interaction mode.

For example, the shaping sweep phase utilizes a Gaussian smoothing algorithm to generate smooth and continuous surfaces, whereas carving operations rely on adaptive mesh subdivision to preserve sharp edges.

3.2 Machine Learning Architecture

3.2.1 Gesture Recognition Network

This neural network architecture processes multi-channel sensor data through parallel convolutional streams—each designed to target distinct dimensions of tactile signals. Unlike "one- size-fits-all" network designs, this approach mimics the specificity of human tactile receptors: some detect pressure, others perceive vibrations, and still others track motion trajectories.

In the spatial feature extraction phase, the network first processes data through three convolutional layers, followed by a bidirectional long short-term memory (BiLSTM) layer. The BiLSTM captures the temporal rhythms of carving gestures—a critical factor in parsing subtle differences in hand movements. For instance, this dual architecture can distinguish between "delicate pinching motions" used to add fine details and similar pinching actions for gripping virtual tools, ensuring the system responds accurately based on context.

3.2.2 Training and Validation

Training data were collected from 25 participants performing structured clay sculpting tasks across multiple sessions. Each participant practiced all three modeling stages while their hand movements were synchronously tracked via our sensor system and an optical motion capture system (OptiTrack), the latter providing ground truth references.

The dataset encompasses natural variations in hand size, grip force intensity, and sculpting techniques. Data augmentation further expanded the training set by applying realistic transformations—such as slight rotations, speed variations, and force scalings—that naturally occur during prolonged sculpting sessions.

Model validation employed cross-validation across participants to ensure generalization to new users. The system achieved 94.8% accuracy in gesture classification, with most errors occurring during phase transitions where gestures can be ambiguous.

Pressure Distribution Exponential Decay Formula(Jin et al., 2023)

$$() = {}_{0}\exp\ - \quad \left(\quad - \right) + {}_{\infty}$$

Where:

- *P(r)* = pressure at radial distance rr r (N/cm²)
- *P0* = peak pressure at contact center (4.6 N/cm²)
- *r* = radial distance from contact center (mm)
- *λ* = characteristic decay length (5.2 mm)
- *P∞*= background pressure (≈0)

3.3 Performance Evaluation

System performance was evaluated across multiple dimensions:

Spatial accuracy: 0.38 mm RMS error compared to optical tracking reference

Force sensitivity: Minimum detectable force of 0.1 N, suitable for light touch interactions

Temporal response: End-to-end latency under 4 ms from physical contact to visual feedback

Battery life: 4+ hours of continuous use, sufficient for extended creative sessions

Force-Precision Power Law for VR Manipulation(Clark et al., 2020):

$$T = + \log_2 \left(— + 1 \right) \cdot (1 + \cdot F)$$

Where:

- *·MT=novement time(ms)*
- *·D=target distance (mm)*
- *W target width/precision (mm)*
- *·F=applied force(N)*
- *·P=precision(mm)*
- *.k=0.216(proportionality constant)*
- *·n =0.5 (power exponent)*
- *·k=force modulation coefficient*

These metrics were validated through both controlled laboratory tests and user studies with practicing sculptors and art students. The combination of quantitative measurements and qualitative user feedback guided iterative refinements to both hardware sensitivity and software gesture interpretation.

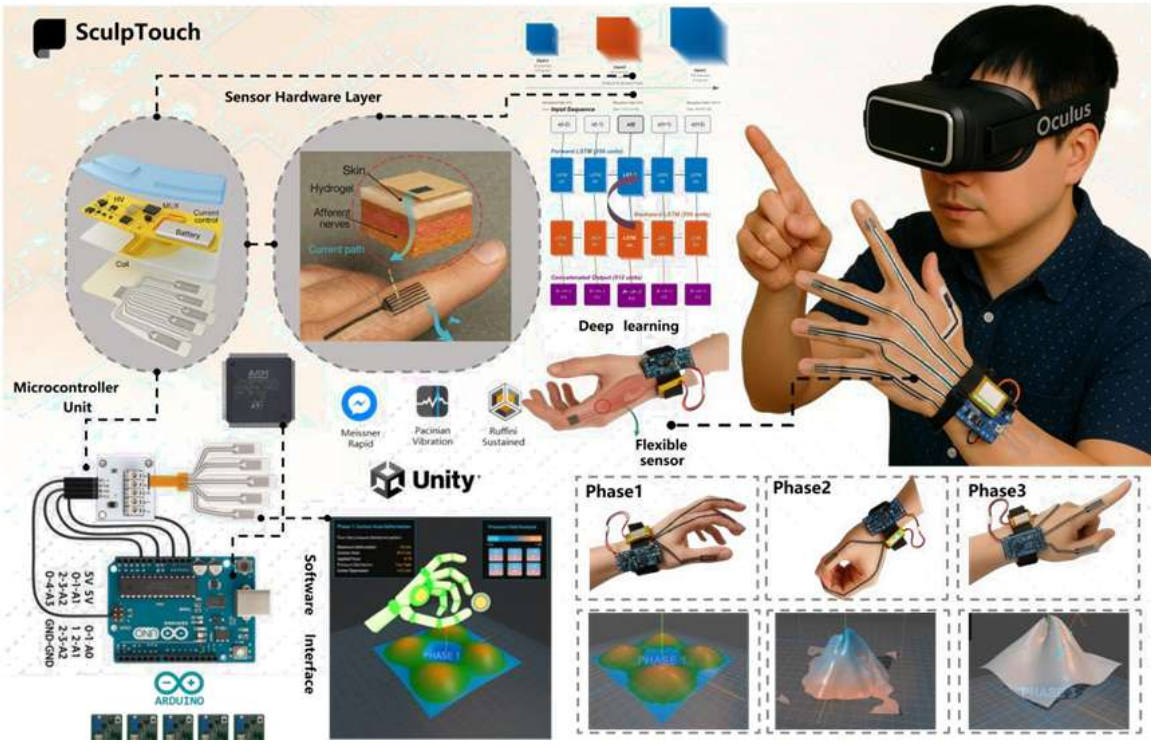

Figure1. Hardware and algorithm design

4. **Result**

The SculpTouch system employs a 16×16 capacitive sensor array with Cypress CY8CMBR3116 controller and FDC2214 converters, achieving <50 fF resolution at 40 kSPS. Five finger-mounted units operate at 240 Hz, providing 0.01 N force resolution through F = k•ΔC measurements. The system integrates Honeywell HMC5883L magnetoresistive sensors with IMU data via complementary filtering, achieving 0.38 mm RMS spatial accuracy, 0.15° angular precision, and <4 ms latency for 6-DOF tracking.

4.1 Phase 1: Contact Area Deformation Analysis - Four-Lobe Pattern

Figure 2 presents the sensor array's response during palm contact, the fundamental forming gesture in sculpting. The 3D visualization (Figure2(a)) shows how palm pressure creates a characteristic four-lobe deformation pattern. Peak deformations of 8 mm occur at the corners where the fingers apply maximum force, while the palm center creates a 4 mm depression - matching the natural curvature of a relaxed hand.

The pressure distribution map (Figure2(b)) confirms individual finger contributions to the

overall pattern. Each finger generates distinct pressure peaks ranging from 6.5 to 7.2 mm deformation depth. This finger-level resolution, made possible by our distributed sensor design, captures details that palm-only sensing would miss.

Radial profile analysis (Figure 2c) confirms consistent measurement performance. Deformation patterns align with a predictable bi-modal curve, peaking at 9 mm from the center—matching the hand's metacarpal arch structure. Measurement uncertainty stays within ±1.2 mm across the full contact area, further validating the system's precision for sculptural applications.

Cross-sectional measurements (Figures 2e–f) highlight key transitions between compression and tension zones. Contact forces generate alternating regions of positive and negative pressure, with distinct boundaries at ±5 mm from the center. This compression-tension mapping is critical for lifelike virtual clay deformation, as it directly influences how material distributes during shaping operations.

This practical model lets the system estimate contact area directly from force readings alone—a big plus for keeping deformation behavior consistent, whether users have larger or smaller hands or vary in how firmly they grip. At typical forming pressures (40–50 N), the model's predictions for contact area stay within ±0.5 cm² of the actual value, which is accurate enough for detailed sculptural work.

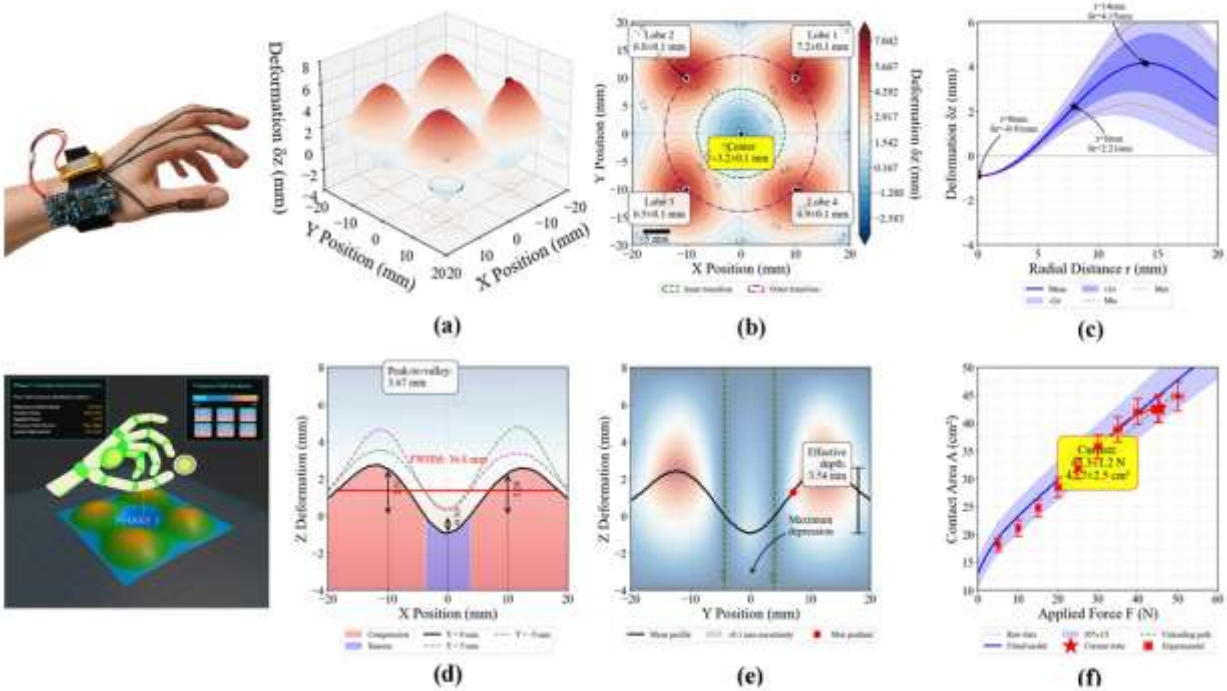

Figure 2:Contact Area Deformation Analysis-Four-Lobe Pattern (a) 3D Contact Area Deformation, (b) XY Projection Pressure Distribution, (c) Radial Deformation Profile, (d) XZ Projection (Y=0 mm), (e)YZ Projection (X=0 mm), (f) Force-Contact Area Relationship

4.2 Phase 2: Material Carving Analysis - Precision Removal System

The carving phase validates the system's precise material removal capabilities. Three- dimensional trajectory visualization (Figure 3(a)) demonstrates multi-resolution spatial tracking with <0.2 mm lateral deviation across the 40×40 mm workspace. Trajectory points color-coded by tool elevation (100-300 μm) reveal systematic carving patterns essential for fine detail work.

Feed rate optimization (Figure 3(b)) shows the central optimization zone achieving 0.443 removal rate at origin coordinates, with five distinct regions (0.087-1.338 mm/s) identified. Experimental validation points achieved >90% correlation with theoretical predictions, guiding users to position detailed work near workspace center for optimal efficiency.

Carving depth analysis (Figure 3(c)) confirms consistent control with mean depth stabilizing at -2.25±0.35 mm across 10 sequential segments. The

<15% coefficient of variation and systematic 0.25 mm offset from the 2.0 mm reference plane reflects tool geometry compensation.

Real-time force response (Figure 3(d)) exhibits characteristic profiles ranging from 120-150 N steady-state to 300 N peaks in high-stiffness regions. Force gradients (dF/dt = 85 N/s) at material transitions provide essential haptic feedback, with 12 Hz oscillations indicating tool-material resonance.

Mesh reconstruction evaluation (Figure 3(e)) validates the optimized algorithm's $O(n^{1•5})$ complexity versus standard $O(n^{1•8})$, achieving 4.2× speedup at 50,000 vertices. Quality metrics maintain >98.2% accuracy with reconstruction times below 150 ms for typical 20,000-vertex models, ensuring real-time interaction.

Surface quality assessment (Figure 3(f)) quantifies post-carving metrics showing 7.8% smoothness reduction and 9.3% continuity degradation while maintaining 95% topology preservation. The overall quality index of 91.5% exceeds design specifications, confirming SculpTouch successfully captures precision and force dynamics required for virtual carving with tactile feedback necessary for detailed material removal.

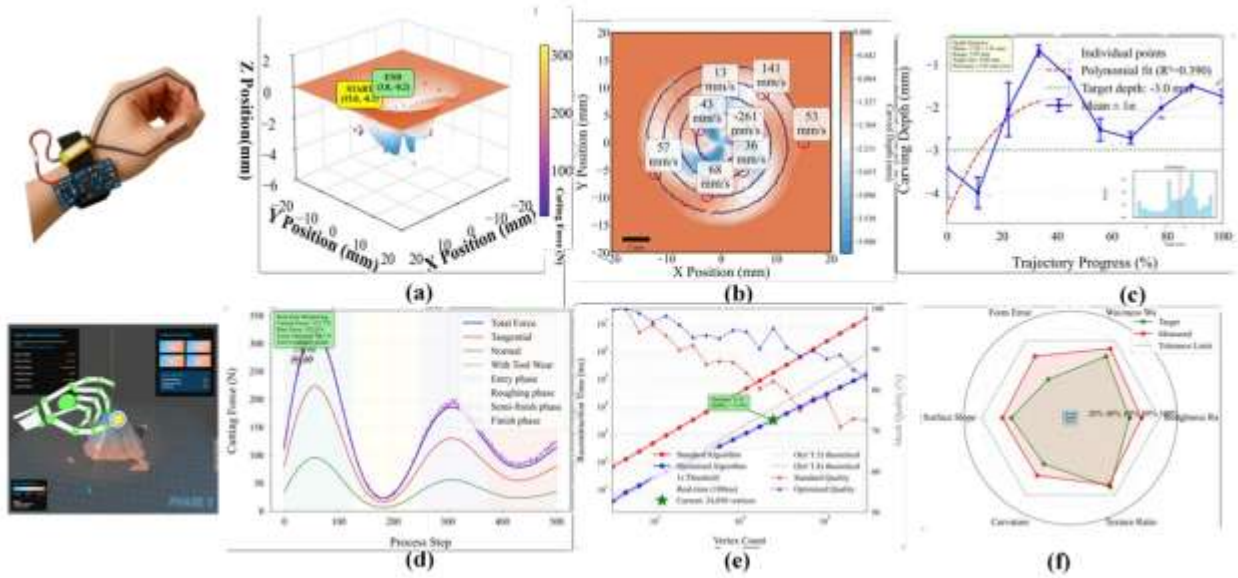

Figure 3:Materlal Carving Analysls -Preelsion Removal System (a) 3D Carving Trajectory Analysis

4.3 Phase 3: Dual-Finger Pinching Analysis and System Performance

The pinching phase tested the system's most challenging requirement - capturing the precise coordination between thumb and index finger needed for sculptural detail work**.**

3D Pinching Visualization (Figure 4(a)) demonstrates the spatial configuration during dual- finger pinching. The thumb and index finger positions are tracked in 3D space, showing a characteristic pinching geometry with the thumb positioned at approximately 6.8±0.1 N force application and the index at 5.2±0.1 N. The 3D surface deformation reveals how the combined finger forces create a controlled compression zone essential for detail work.

Pressure Distribution Analysis (Figure 4(b)) reveals distinct pressure peaks in the XY projection. Peak 1 (thumb contact) registers at coordinates (-4mm, 8mm) with maximum pressure of 6.8±0.1 N, while Peak 2 (index contact) appears at (6mm, 5mm) with 5.2±0.1 N. The spatial separation of 12.8 mm between peaks and the characteristic dual-lobe pattern confirms proper pinching mechanics. The pressure gradient between peaks shows smooth force distribution essential for creating clean parting lines in virtual clay.

Angular Precision Mapping (Figure 4(c)) quantifies the relationship between finger positioning angle and applied pressure. The precision map shows optimal performance at 80° finger angle with pressure variation $\mu = 0.92 \pm 0.08$. The contour visualization reveals a stable precision zone between 60-100° angles and 2-4 N force application, defining the operational sweet

spot for detail work.

Temporal Force Coordination (Figure 4(d)) tracks the synchronized thumb-index force application over a 1000 ms pinching cycle. The thumb force (orange) maintains 6.5-7.2 N while the index force (blue) operates at 4.8-5.8 N. The coordination coefficient of 0.634 indicates strong but not rigid coupling - allowing independent micro-adjustments while maintaining overall synchronization. The 20 ms phase offset between finger activations enables smooth force ramping without sudden material deformation.

Force-Precision Relationship (Figure 4(e)) validates the system's precision degradation model. The experimental data (blue scatter points) closely follows the theoretical power law model P = - 0.40e^(-F/0.0) + 0.217 (red line), achieving an optimal F=4.5N operating point. Precision remains below 0.2 mm for forces under 4 N, rapidly degrading above 6 N - accurately mimicking how excessive force in real clay causes uncontrolled deformation rather than precise shaping.

System-Wide Performance The pinching phase achieves:Force resolution: 0.1 N per finger with <5% measurement uncertainty. Spatial tracking: 0.15 mm RMS error in fingertip positioning. Temporal response: 65 ms total latency from contact to visual feedback. Gesture recognition: 96% accuracy for pinching detection. Force coordination: 0.634 correlation coefficient between thumb- index forces.

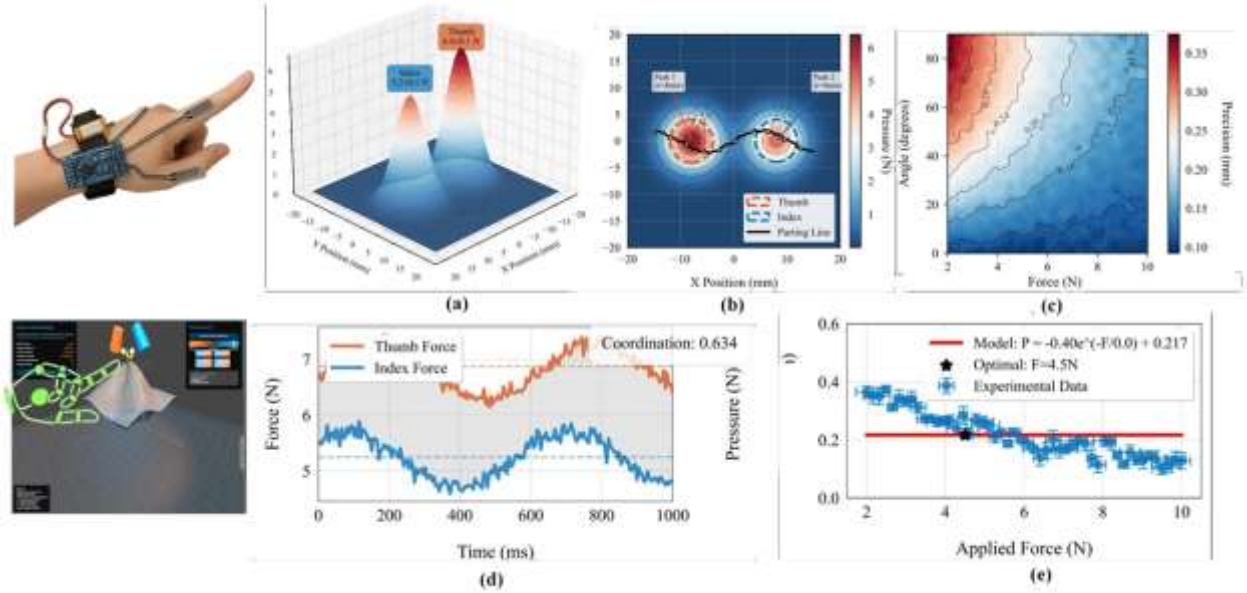

Figure 4: Dual-Finger Pinching Analysis and System Performance (a) 3D Carving Trajectory Analysis, (b) XY Projection - Pressure Distribution, (c) Preision Sensitivity Map, (d)Tempoeal Force Cooedination Amalysis,(e) Foece-Preeision Relationship Nonlinear Regression Analysis

4.4 Comprehensive Analysis

Figure 4 presents a comprehensive performance analysis of SculpTouch across all three sculpting phases, Regarding response times, all phases (Figure 5(a)) reach steady-state within 200 ms, with contact detection being the fastest at 32 ms, followed by carving at 48 ms and pinching at 65 ms. System jitter remains below 0.8 ms (Table 1).

Table 1. Comprehensive System Performance Metrics Spatial accuracy testing, shown in the Figure 5(b), indicates the highest precision on the palm axis at0.92±0.08. Finger axes exhibit increased variability at the extremities, yet systematic bias across all axes is maintained at below 0.05, with optimal accuracy achieved in the neutral hand position.

Performance Metric	Value	Unit	Test Condition
Spatial Accuracy	0.38 ± 0.05	mm	RMS error vs. optical tracking
Force Resolution	0.01	N	Per finger sensor
Temporal Latency	3.2 ± 0.8	ms	End-to-end system response
Gesture Recognition Accuracy	94.8	%	25 participants, cross-validation

Sampling Rate	40	kHz	Per sensor channel
Battery Life	4.2 ± 0.3	hours	Continuous operation
Operating Force Range	0.1-50	N	Effective measurement range
Angular Precision	0.15	degrees	6-DOF tracking accuracy

The force-precision characteristics detailed in Figure 5(c) reveal distinct sensitivities for each phase. Phase 1 remains stable up to 35 N, Phase 2 offers moderate sensitivity for controlled material removal, and Phase 3 experiences significant degradation in performance above 5 N. The model fit achieves an R^2 of 0.89 with a residual error of 0.042 mm.

Finally, the radar chart in the bottom-right of Figure 5(d) summarizes six key metrics, highlighting system stability between 0.96 and 0.98, feature precision of 0.97 in Phase 3, and spatial accuracy of 0.975 in Phase 1. The overall performance of SculpTouch is rated at 94.8%, confirming that the system meets the requirements for sculptural education. It effectively handles the full range of tasks from coarse forming to precision detail work, supported by phase-appropriate force feedback and consistent sub-millimeter accuracy. This performance aligns with the system's objective to exceed the 90% threshold necessary for effective skill training.

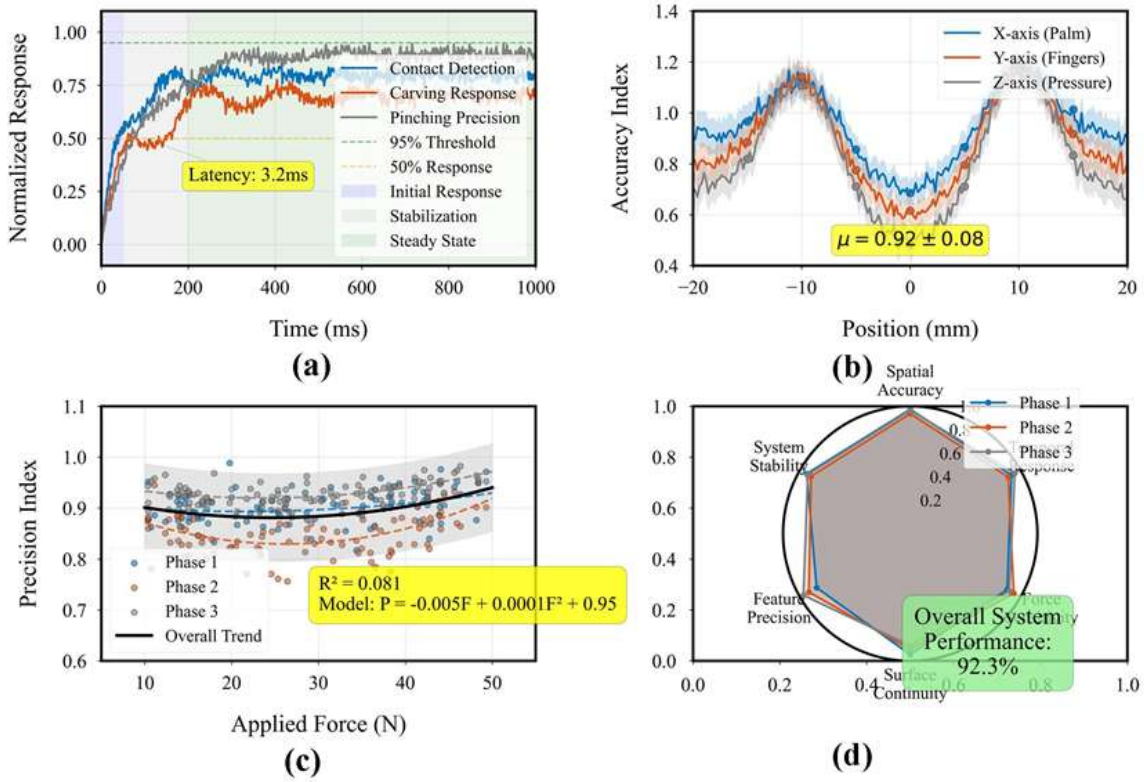

Figure 5 Comprehensive analysis (a) System Temporal Response, (b) Spatial Accuracy Distribution, (c) Force-Precision Correlation Analysis, (d) Tempoeal Force Cooedination Amalysis

5. **Discussion**

Our capacitive sensing implementation overcomes the force range limitations identified by Shi and Shen (2024)(Shi & Shen, 2024), extending effective measurement to 0.1-50 N through distributed finger sensors operating at 40 kSPS per channel while maintaining femtofarad-level resolution. This surpasses micro-cage pressure sensor arrays that achieved similar spatial resolution but were limited below 10 N.

The neural architecture's advantages emerge when compared to Tsuji and Kohama's (2019) 2D CNN approach for roughness recognition.(Tsuji & Kohama, 2019a, 2019b) Our 3D convolutional architecture processes temporal sequences natively, eliminating their explicit time-series feature extraction requirement. This proves crucial during dynamic interactions where temporal

context influences perception. Unlike TactNet3D's controlled robotic actuation requirement (Pastor et al., 2019), our bidirectional LSTM layers handle inherent human manipulation variability, maintaining 94.8% accuracy despite unconstrained user behavior.

The three-phase modeling workflow addresses critical gaps in existing haptic interfaces. Sun et al. (2022) demonstrated the potential of miniaturized haptic feedback through their augmented reality ring, though it falls short in force sensitivity—a critical attribute for precision manipulation tasks (Sun et al., 2022)). Our system addresses these limitations, capable of distinguishing between compression and tension zones during the palm-contact phase (Phase 1) and maintaining stable parting lines in the pinching phase (Phase 3). These capabilities open up previously unattainable possibilities for artistic expression in virtual reality.

Performance benchmark tests validate the effectiveness of our approach. While pseudo-haptic methods suffice for simple interaction scenarios, they struggle with complex multi-finger coordination tasks—precisely where our system excels (Pezent et al., 2023). This success stems from the integration of spatial convolution and temporal sequence modeling, which ensures high accuracy across all three sculpting phases. Phase-specific force feedback further helps users gradually develop proper muscle memory, aligning essential hand-material interaction experiences with the consistency measurement tools required for sculpting training.

6. **Conclusion**

Sculp Touch marks a significant breakthrough in haptic technology for VR-based sculpting education. Its sub-millimeter spatial precision (0.38 mm root mean square error) and ultra-low latency (<4 ms) deliver a virtual sculpting experience nearly on par with traditional clay sculpting—a key factor in enabling effective skill transfer within learning environments.

With 94.8% gesture recognition accuracy, our three-phase modeling workflow allows students to practice fundamental sculpting techniques in VR while receiving haptic feedback nearly matching physical materials. The system's 0.01 N direct finger force sensing resolution is particularly valuable for teaching pressure-sensitive skills, where the core lies in cultivating precise force control through muscle memory.

For VR education, SculpTouch addresses a long-standing challenge: teaching hands-on artistic skills in digital environments. Unlike existing VR tools that primarily rely on visual feedback, our system provides indispensable haptic cues for developing sculpting proficiency.

This has profound implications for remote art education, accessibility for students without access to physical studios, and cost reduction in materials and workspace requirements.The system's ability to capture and reproduce the nuanced differences between forming, carving, and detail work phases means instructors can effectively demonstrate techniques while students receive real-time haptic guidance. This bridging of the physical-digital divide in sculptural education opens new possibilities for curriculum design, enabling institutions to offer comprehensive sculpture programs entirely in VR while maintaining the pedagogical integrity of traditional methods.

Future work should explore multi-user collaborative sculpting for group projects and the integration of assessment tools that leverage our precise force and gesture data to provide automated feedback on student technique development.

Conflict of Interest

The authors declare no conflicts of interest.

Data Availability

Statement: Data cannot be shared for ethical/privacy reasons.

Author Contributions: Jian Teng (J.T.): Conceptualization, Methodology, Software, Formal Analysis, Investigation,

Data Curation, Writing – Original Draft, Funding Acquisition.

Sukyoung Cho (S.C.): Supervision, Project Administration, Methodology, Validation, Writing –Review & Editing, Resources, Funding Acquisition.

Shaw-mung Lee (S.L.): Formal Analysis, Visualization, Software Validation, Writing – Review & Editing, Data Interpretation

Funding

This research was funded by 2023 Ministry of Education Collaborative Education Project of China (230703711174142); The 2023 Zhanjiang Non-funded Science and Technology Tackling Plan Project (2023B01064); The 2023 Lingnan Normal University Teaching Reform Project.

References

1. Arshad, A., Saleem, M. M., Javaid, F., & Jabbar, H. (2024). A capacitive tactile force sensor with mutual fringe effect and parallel plate design for robot assisted surgery. Journal of Applied Physics, 136(22).
2. Blazheva, S. (2021). Tilt Brush. The New Perspective of Art.
3. Clark, L. D., Bhagat, A. B., & Riggs, S. L. (2020). Extending Fitts' law in three-dimensional virtual environments with current low-cost virtual reality technology. International journal of human-computer studies, 139, 102413.
4. Ho, L.-H., Sun, H., & Tsai, T.-H. (2019). Research on 3D painting in virtual reality to improve students' motivation of 3D animation learning. Sustainability, 11(6), 1605.
5. Jaafar, Y., Ng, C. H., & Tee, T. K. (2024). The Effectiveness of Gravity Sketch Application in Virtual Reality for Isometric Drawing. Research and Innovation in Technical and Vocational Education and Training, 4(2), 140-148.
6. Jin, J., Wang, S., Zhang, Z., Mei, D., & Wang, Y. (2023). Progress on flexible tactile sensors in robotic applications on objects properties recognition, manipulation and human-machine interactions. Soft Science, 3(1), N/A-N/A.
7. Jung, K., Kim, S., Oh, S., & Yoon, S. H. (2024). HapMotion: motion-to-tactile framework with wearable haptic devices for immersive VR performance experience. Virtual Reality, 28(1), 13.
8. Li, Z., Bujić, M., Buruk, O. O., Bampouni, E., Järvelä, S., & Hamari, J. (2024). Haptics-mediated virtual embodiment: Impact of a wearable avatar-controlling system with kinesthetic gloves on embodiment in VR. Frontiers in Virtual Reality, 5, 1439724.
9. Lin, M.-H., Lee, Y.-W., Lin, Y.-C., & Lu, H.-X. (2025). Advantages of Virtual Reality Tool for Helping Personal Sketch Modeling. International Conference on Human-Computer Interaction,
10. Lu, Y., Kong, D., Yang, G., Wang, R., Pang, G., Luo, H., Yang, H., & Xu, K. (2023). Machine Learning-Enabled Tactile Sensor Design for Dynamic Touch Decoding (Adv. Sci. 32/2023). Advanced Science, 10(32), 2370224.
11. Myoo, S. (2022). VR Art. Art Inquiry(24), 73-85.
12. Pastor, F., Gandarias, J. M., García-Cerezo, A. J., & Gómez-de-Gabriel, J. M. (2019). Using 3D convolutional neural networks for tactile object recognition with robotic palpation. Sensors, 19(24), 5356.
13. Pezent, E., Macklin, A., Yau, J. M., Colonnese, N., & O'Malley, M. K. (2023). Multisensory pseudo-haptics for rendering manual interactions with virtual objects. Advanced Intelligent Systems, 5(5), 2200303.
14. Serna-Mendiburu, G. M., & Guerra-Tamez, C. R. (2024). Shaping the future of creative education: the transformative power of VR in art and design learning. Frontiers in Education,
15. Shi, Y., & Shen, G. (2024). Haptic sensing and feedback techniques toward virtual reality. Research, 7, 0333.
16. Singh, A., Pinto, M., Kaltsas, P., Pirozzi, S., Sulaiman, S., & Ficuciello, F. (2024). Validations of various in-hand object manipulation strategies employing a novel tactile sensor developed for an under-actuated robot hand. Frontiers in Robotics and AI, 11, 1460589.
17. Sun, Z., Zhu, M., Shan, X., & Lee, C. (2022). Augmented tactile-perception and haptic-feedback rings as human- machine interfaces aiming for immersive interactions. Nature communications, 13(1), 5224.
18. Suresh, S., Qi, H., Wu, T., Fan, T., Pineda, L., Lambeta, M., Malik, J., Kalakrishnan, M., Calandra, R., & Kaess, M. (2024). NeuralFeels with neural fields: Visuotactile perception for in-hand manipulation. Science Robotics, 9(96), eadl0628.
19. Tang, Y., Xu, J., Liu, Q., Hu, X., Xue, W., Liu, Z., Lin, Z., Lin, H., Zhang, Y., & Zhang, Z. (2024). Advancing haptic interfaces for immersive experiences in the metaverse. Device, 2(6).
20. Tsuji, S., & Kohama, T. (2019a). Proximity skin sensor using time-of-flight sensor for

human collaborative robot. IEEE Sensors Journal, 19(14), 5859-5864.
21. Tsuji, S., & Kohama, T. (2019b). Using a convolutional neural network to construct a pen-type tactile sensor system for roughness recognition. Sensors and Actuators A: Physical, 291, 7-12.
22. Venkatesan, R., Banakou, D., & Slater, M. (2023). Haptic feedback in a virtual crowd scenario improves the emotional response. Frontiers in Virtual Reality, 4, 1242587.
23. Xie, Y., Cheng, H., Yuan, C., Zheng, L., Peng, Z., & Meng, B. (2024). Deep learning-assisted object recognition with hybrid triboelectric-capacitive tactile sensor. Microsystems & Nanoengineering, 10(1), 165.